Bayesian Imaging for Intensity Interferometry with Deep Generative Priors

Biwei Dai
Institute for Advanced Study
November 1 @ Future Prospects of Intensity Interferometry workshop
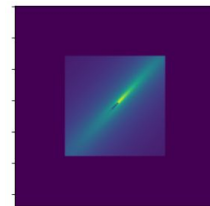
collaborated with Neal Dalal

Phase Retrieval

▷ Intensity interferometer measures the Fourier amplitudes and loses the phase information.

▷ The problem of reconstructing a signal from its Fourier magnitude is known as phase retrieval. This reconstruction problem has a rich history and arises in many areas of engineering and applied physics.

▷ Coherent diffraction imaging:
  ○ Idea introduced in 1950s and 1980
  ○ Phase retrieval algorithms developed in 1970s and 1980s
  ○ First experimental demonstration in 1999
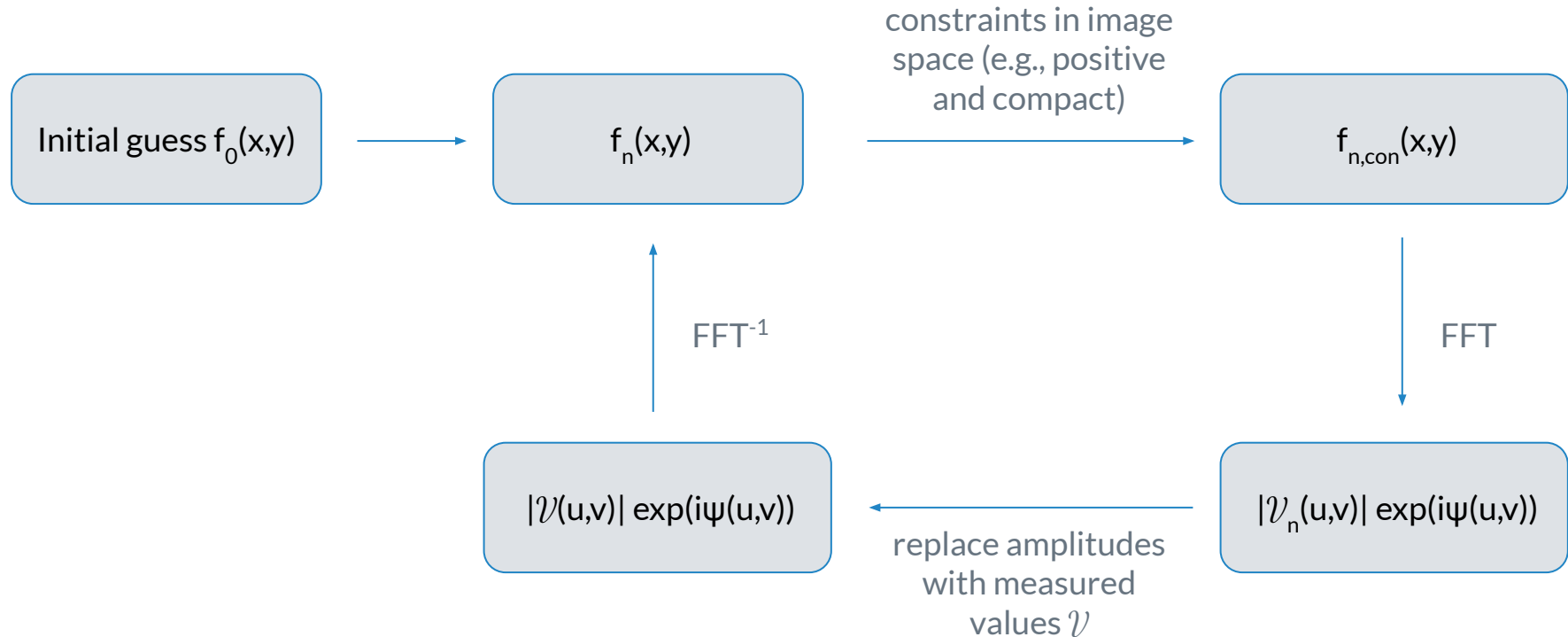

Coherent diffraction imaging
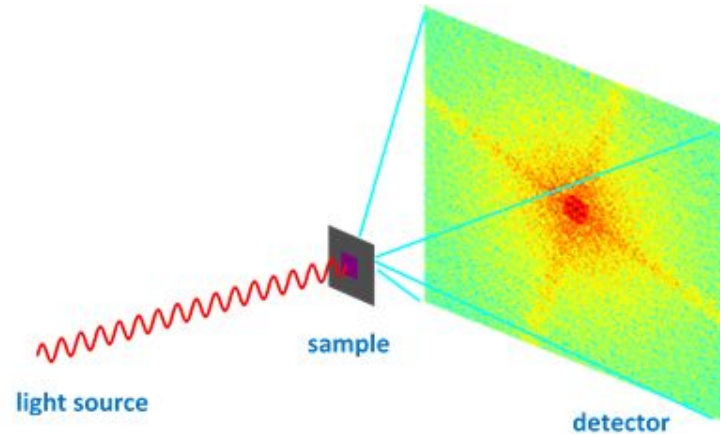
Why is Phase Retrieval possible?

▷ Additional constraints / regularizations / prior information are necessary to retrieve the phases

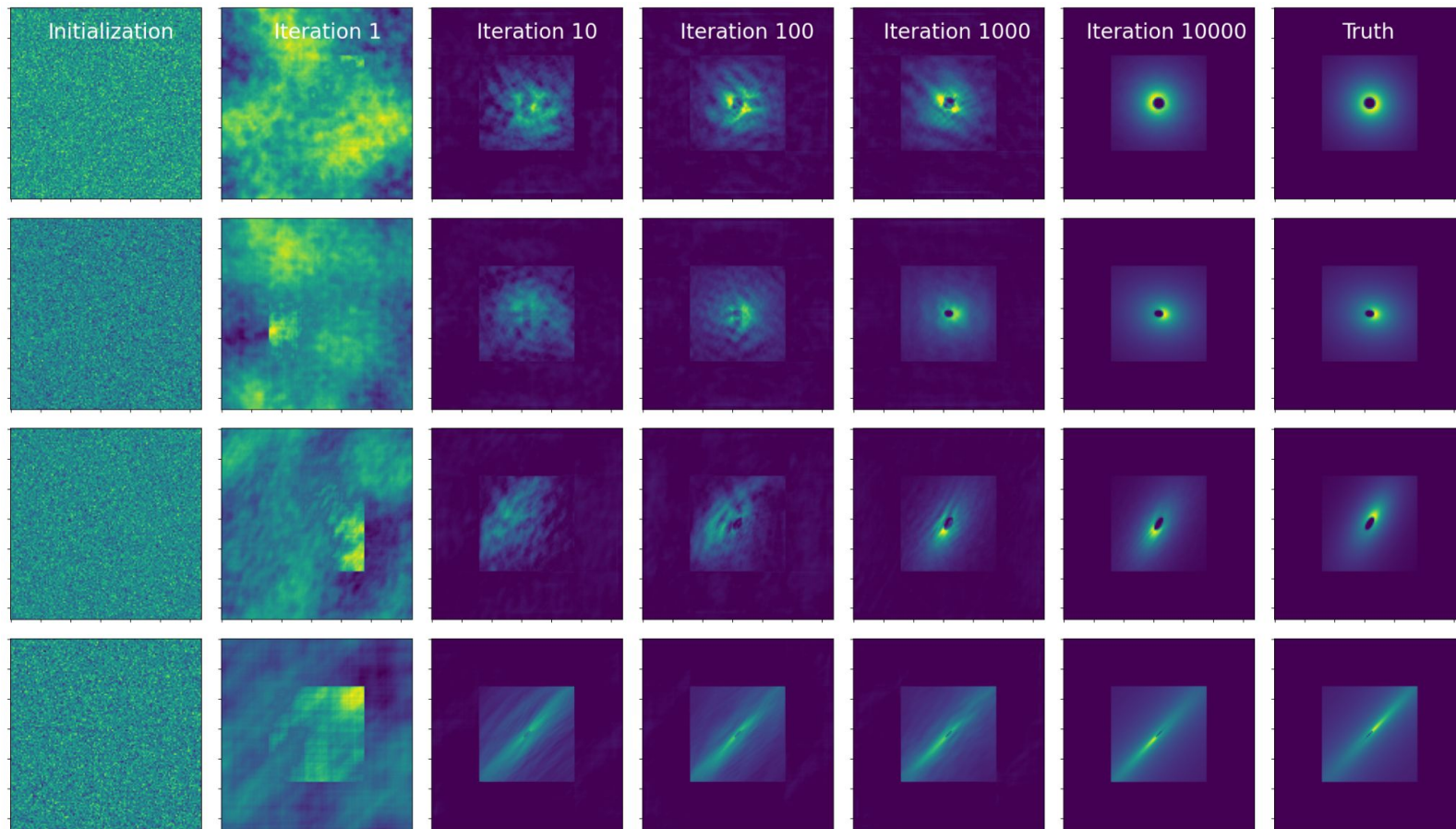   ○ Positivity, smoothness, compactness, etc.

▷ Theorem: the signal can be uniquely reconstructed (up to some trivial transformations such as translation and inversion), if

    ○ the Fourier amplitudes are oversampled by at least a factor of 2 (i.e., pixel value non-zero only at the central $(L/2)^2$ pixels)

    ○ the signal cannot be represented by the convolution of two noncentrosymmetric functions

Iterative phase retrieval algorithm

```
┌─────────────────────┐        ┌─────────────────────┐   constraints in image    ┌─────────────────────┐
│ Initial guess f₀(x,y)│  ───▶  │      fₙ(x,y)        │   space (e.g., positive   │    fₙ,con(x,y)      │
└─────────────────────┘        └─────────────────────┘      and compact)         └─────────────────────┘
```

Initial guess $f_0(x,y)$ → $f_n(x,y)$

constraints in image space (e.g., positive and compact) → $f_{n,con}(x,y)$

FFT^{-1}

FFT

$|\mathcal{V}(u,v)|\exp(i\psi(u,v))$ ← replace amplitudes with measured values $\mathcal{V}$ ← $|\mathcal{V}_n(u,v)|\exp(i\psi(u,v))$

Hybrid input-out (HIO) algorithm

However...

▷ The HIO algorithm assumes
- Oversampling the Fourier amplitudes by at least a factor of 2 (i.e., the image is only non-zero at the central $(L/2)^2$ pixels) (also guarantees unique solution)
- Noiseless data

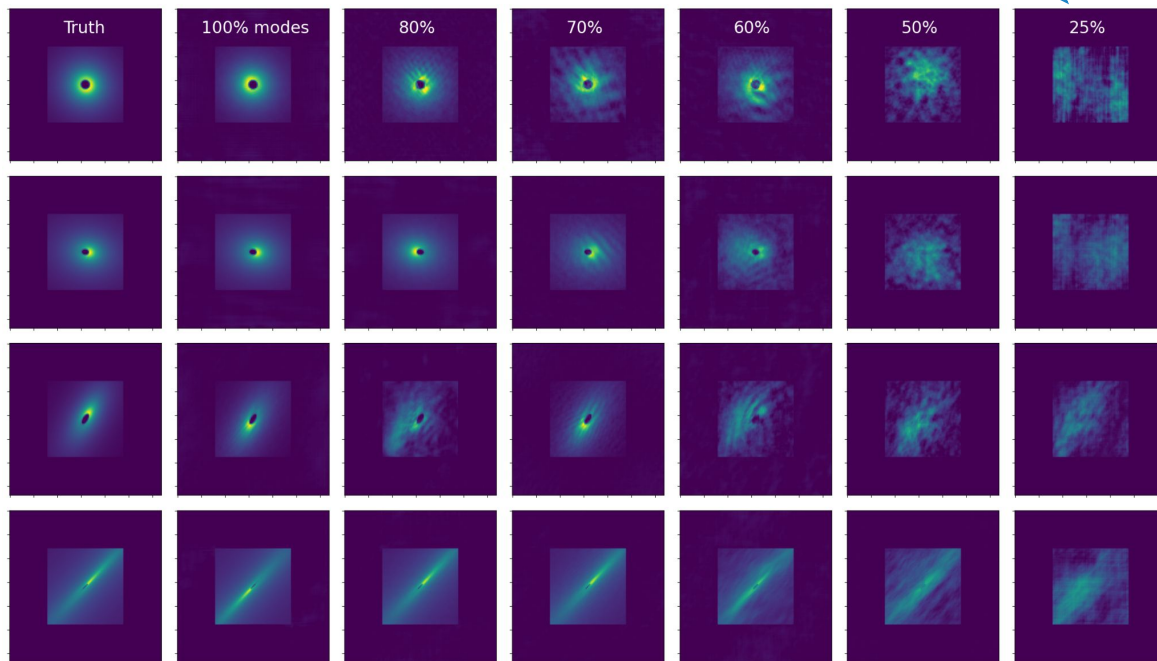▷ In reality, our measurements are
- Sparsely-sampled
- Noisy

However…

▷ The HIO algorithm assumes
  ○ Oversampling the Fourier amplitudes by at least a factor of 2 (i.e., the image is only non-zero at the central $(L/2)^2$ pixels) (also guarantees unique solution)
  ○ Noiseless data

▷ In reality, our measurements are
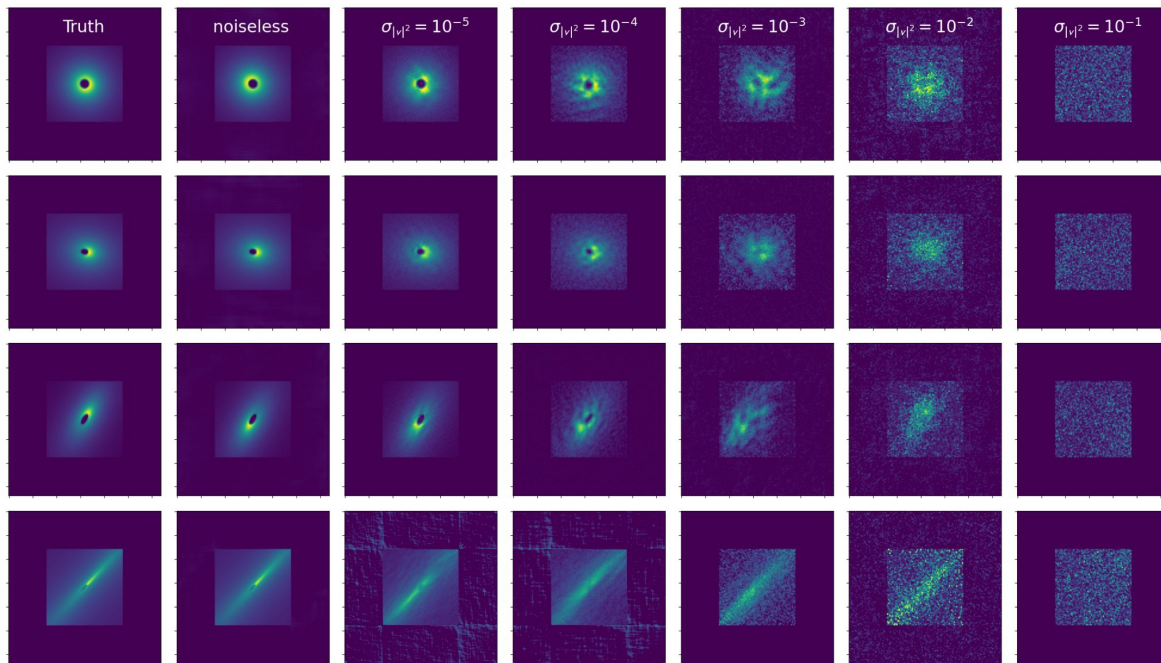 ○ Sparsely-sampled
  ○ Noisy

7

However...

▷ The HIO algorithm assumes
   ○ Oversampling the Fourier amplitudes by at least a factor of 2 (i.e., the image is only non-zero at the central $(L/2)^2$ pixels) (also guarantees unique solution)
   ○ Noiseless data

▷ In reality, our measurements are
   ○ Sparsely-sampled
   ○ Noisy

Phase retrieval in a Bayesian framework

$$\log p(\,\textbf{Image}\mid|\mathcal{V}|^2\,) = \log p(|\mathcal{V}|^2\mid\textbf{Image}\,) + \log p(\textbf{Image}) - \log p(|\mathcal{V}|^2)$$

Likelihood function given by the measurement noise model. Usually approximated with a Gaussian

Prior function. It could either be some constraints or regularizations, or it could be learned from simulations.

- Easily incorporate measurement noise

- Uncertainty quantification with posterior sampling

Choices of prior

▷ HIO algorithm
   ○ Positive pixel values
   ○ Compact object (nonzero at the central $(L/2)^2$ pixels / oversampling the Fourier plane)

▷ The regularizations in EHT image reconstruction (RML algorithm):
   ○ Total flux
   ○ Favors images similar to a "prior image"(a circular Gaussian)
   ○ Sparsity (L1 norm)
   ○ Smoothness (total variation, total squared variation)
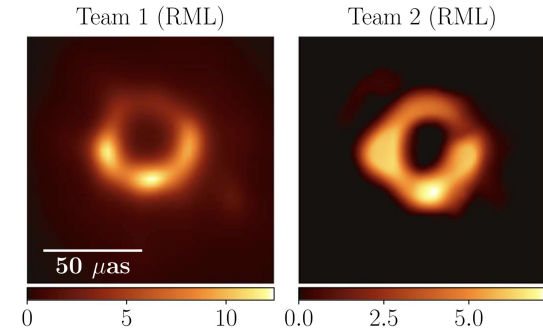
EHT collaboration 2019. [1906.11241]

▷ How to incorporate our physical knowledge (e.g., the AGN disk is thin and roughly follows a Shakura-Sunyaev profile, or predictions from GRMHD simulations) into the prior?

Deep generative priors

▷ A generative model aims to model the underlying probability distribution (our prior distribution) of a dataset, given independently and identically distributed (i.i.d.) samples (e.g., simulations, analytical models).

▷ Score-based diffusion models estimate the gradient of the log density function (score function, ∇ log p).

$$\nabla \log p(\text{Image} \mid |\mathcal{V}|^2) = \nabla \log p(|\mathcal{V}|^2 \mid \text{Image}) + \nabla \log p(\text{Image})$$

Gradient of Gaussian likelihood.

Learned by diffusion model.

Credit: https://yang-song.net/blog/2021/score/
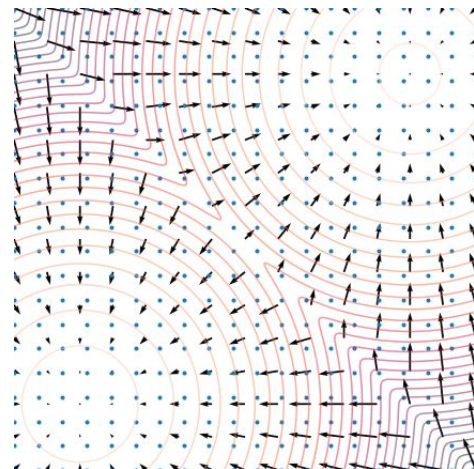
Experiments

We consider two experiment setups:

- Shakura-Sunyaev disk

$$I(R) = I_0 \left[e^{f(R)} - 1 \right]^{-1}$$

$$f(R) = \frac{\nu}{\nu_0(R)} = \left[\left(\frac{R_0}{R} \right)^n \left(1 - \sqrt{\frac{R_{\text{in}}}{R}} \right) \right]^{-1/4}$$

- GRMHD simulations for RIAF (Wong et al. 2022)

Low noise, densely sampled case

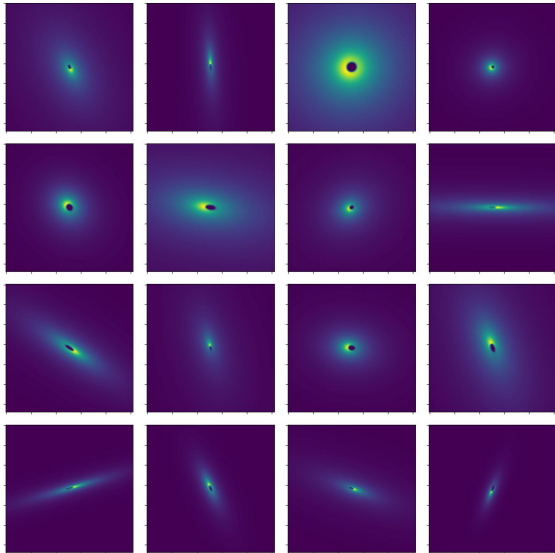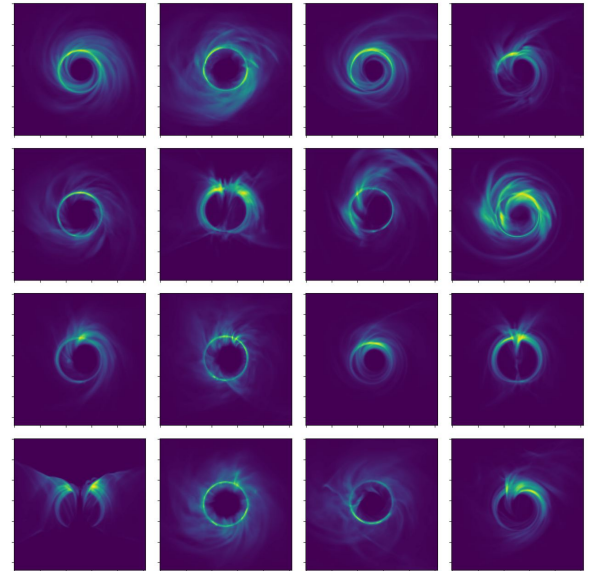▷ The reconstructed images converge to the truth when the noise is low $\sigma_{|v|^{\wedge}2}=10^{-4}$ and the Fourier space is densely sampled.
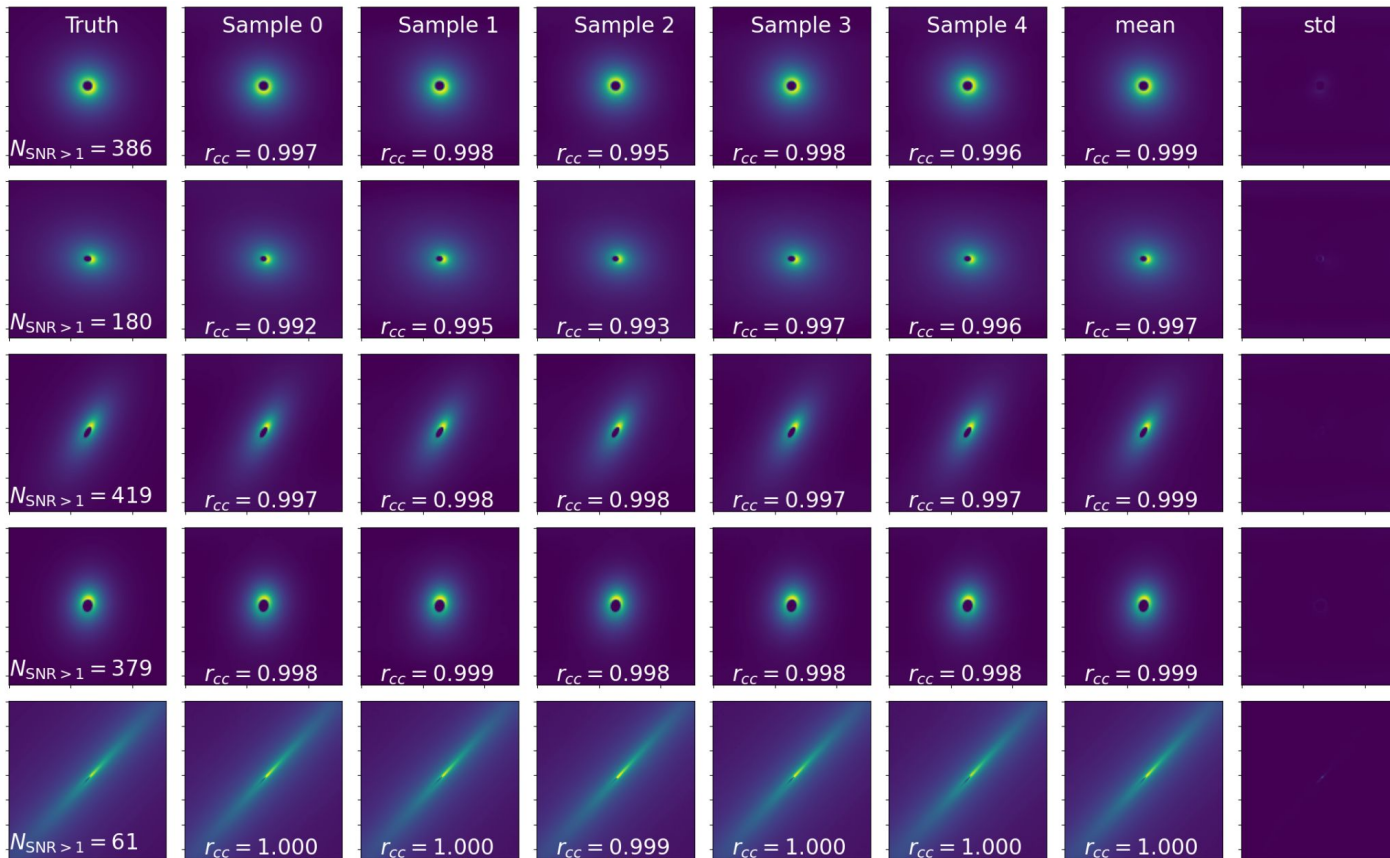
▷ Note that unlike HIO algorithm, here we don't need to oversample the Fourier space. The HIO algorithm fails at this noise level, even though it uses 4 times more measurements.

Truth	Sample 0	Sample 1	Sample 2	Sample 3	Sample 4	mean	std
$N_{\mathrm{SNR}>1}=386$	$r_{cc}=0.997$	$r_{cc}=0.998$	$r_{cc}=0.995$	$r_{cc}=0.998$	$r_{cc}=0.996$	$r_{cc}=0.999$	
$N_{\mathrm{SNR}>1}=180$	$r_{cc}=0.992$	$r_{cc}=0.995$	$r_{cc}=0.993$	$r_{cc}=0.997$	$r_{cc}=0.996$	$r_{cc}=0.997$	
$N_{\mathrm{SNR}>1}=419$	$r_{cc}=0.997$	$r_{cc}=0.998$	$r_{cc}=0.998$	$r_{cc}=0.997$	$r_{cc}=0.997$	$r_{cc}=0.999$	
$N_{\mathrm{SNR}>1}=379$	$r_{cc}=0.998$	$r_{cc}=0.999$	$r_{cc}=0.998$	$r_{cc}=0.998$	$r_{cc}=0.998$	$r_{cc}=0.999$	
$N_{\mathrm{SNR}>1}=61$	$r_{cc}=1.000$	$r_{cc}=1.000$	$r_{cc}=0.999$	$r_{cc}=1.000$	$r_{cc}=1.000$	$r_{cc}=1.000$	

Changing noise levels
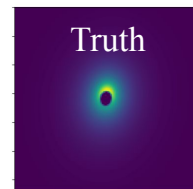
▷ The reconstruction is poorer and the algorithm is less certain with more noise. In the high noise limit, the algorithm essentially generates random samples from the prior.

▷ Sampling the posterior allows us to quantify the uncertainty of the image reconstruction.

Sample 1	Sample 2	Sample 3	Sample 4	Sample 5	mean	std
$\sigma_{|v|^2} = 10^{-3}$						
$N_{SNR > 1} = 184$						
$r_{cc} = 0.999$	$r_{cc} = 0.999$	$r_{cc} = 0.998$	$r_{cc} = 0.999$	$r_{cc} = 0.999$	$r_{cc} = 0.999$	
$\sigma_{|v|^2} = 10^{-2}$						
$N_{SNR > 1} = 18$						
$r_{cc} = 0.997$	$r_{cc} = 0.994$	$r_{cc} = 0.994$	$r_{cc} = 0.997$	$r_{cc} = 0.995$	$r_{cc} = 0.997$	
$\sigma_{|v|^2} = 10^{-1}$						
$N_{SNR > 1} = 7$						
$r_{cc} = 0.975$	$r_{cc} = 0.592$	$r_{cc} = 0.907$	$r_{cc} = 0.789$	$r_{cc} = 0.811$	$r_{cc} = 0.878$	
$\sigma_{|v|^2} = 10^{0}$						
$N_{SNR > 1} = 1$						
$r_{cc} = 0.726$	$r_{cc} = 0.600$	$r_{cc} = 0.823$	$r_{cc} = 0.879$	$r_{cc} = 0.538$	$r_{cc} = 0.760$	
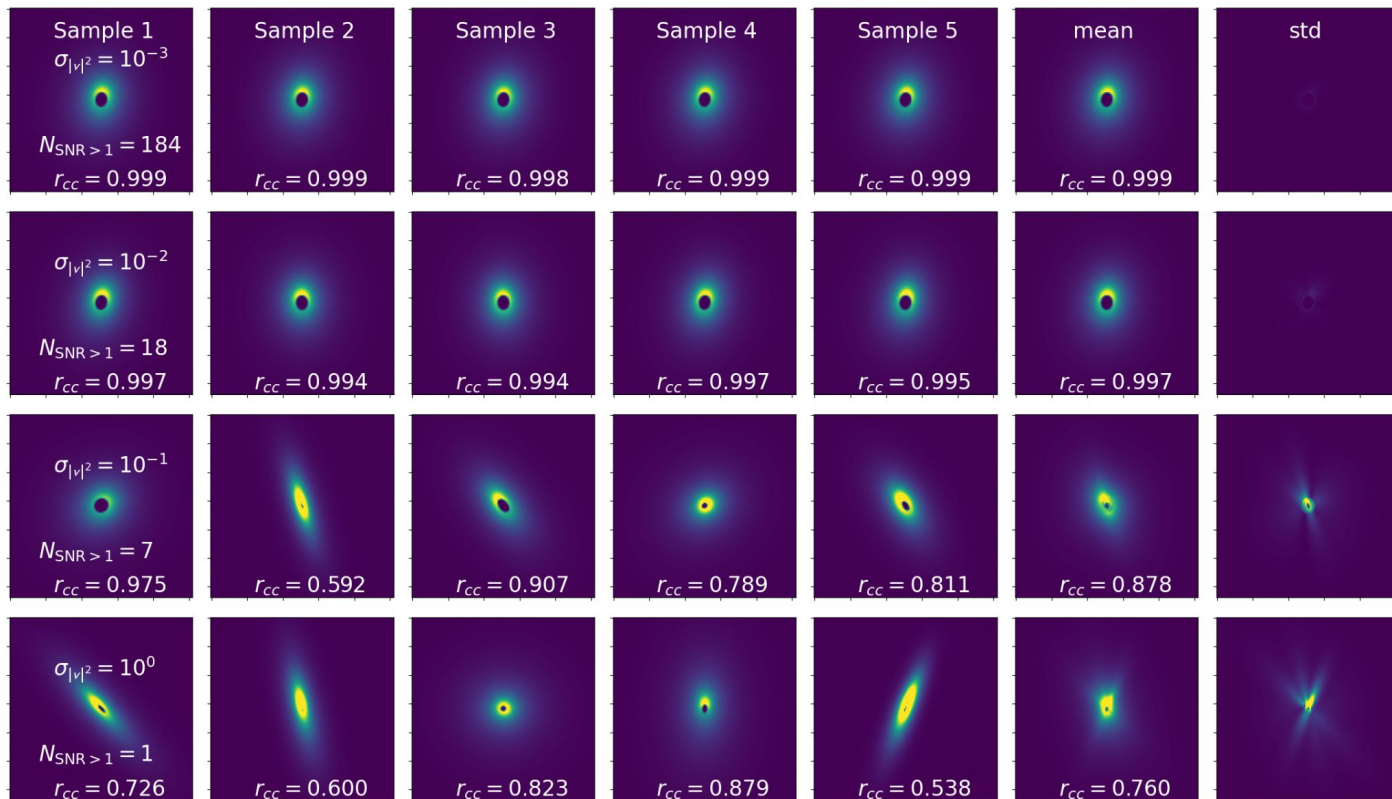
Changing UV coverage
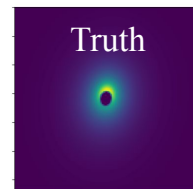
▷ Apply a random mask in the Fourier space. The noise level is fixed at $\sigma_{|v|^2}=10^{-2}$

▷ Preliminary results: the model works well within the UV coverage range we tested.

Truth

Sample 1 100 % modes	Sample 2	Sample 3	Sample 4	Sample 5	mean	std
$N_{SNR>1}=18$ $r_{cc}=0.997$	$r_{cc}=0.994$	$r_{cc}=0.994$	$r_{cc}=0.997$	$r_{cc}=0.995$	$r_{cc}=0.997$	
80 % modes $N_{SNR>1}=15$ $r_{cc}=0.996$	$r_{cc}=0.994$	$r_{cc}=0.994$	$r_{cc}=0.996$	$r_{cc}=0.994$	$r_{cc}=0.996$	
50 % modes $N_{SNR>1}=6$ $r_{cc}=0.995$	$r_{cc}=0.988$	$r_{cc}=0.988$	$r_{cc}=0.996$	$r_{cc}=0.996$	$r_{cc}=0.997$	
20 % modes $N_{SNR>1}=0$ $r_{cc}=0.993$	$r_{cc}=0.981$	$r_{cc}=0.982$	$r_{cc}=0.996$	$r_{cc}=0.804$	$r_{cc}=0.987$	
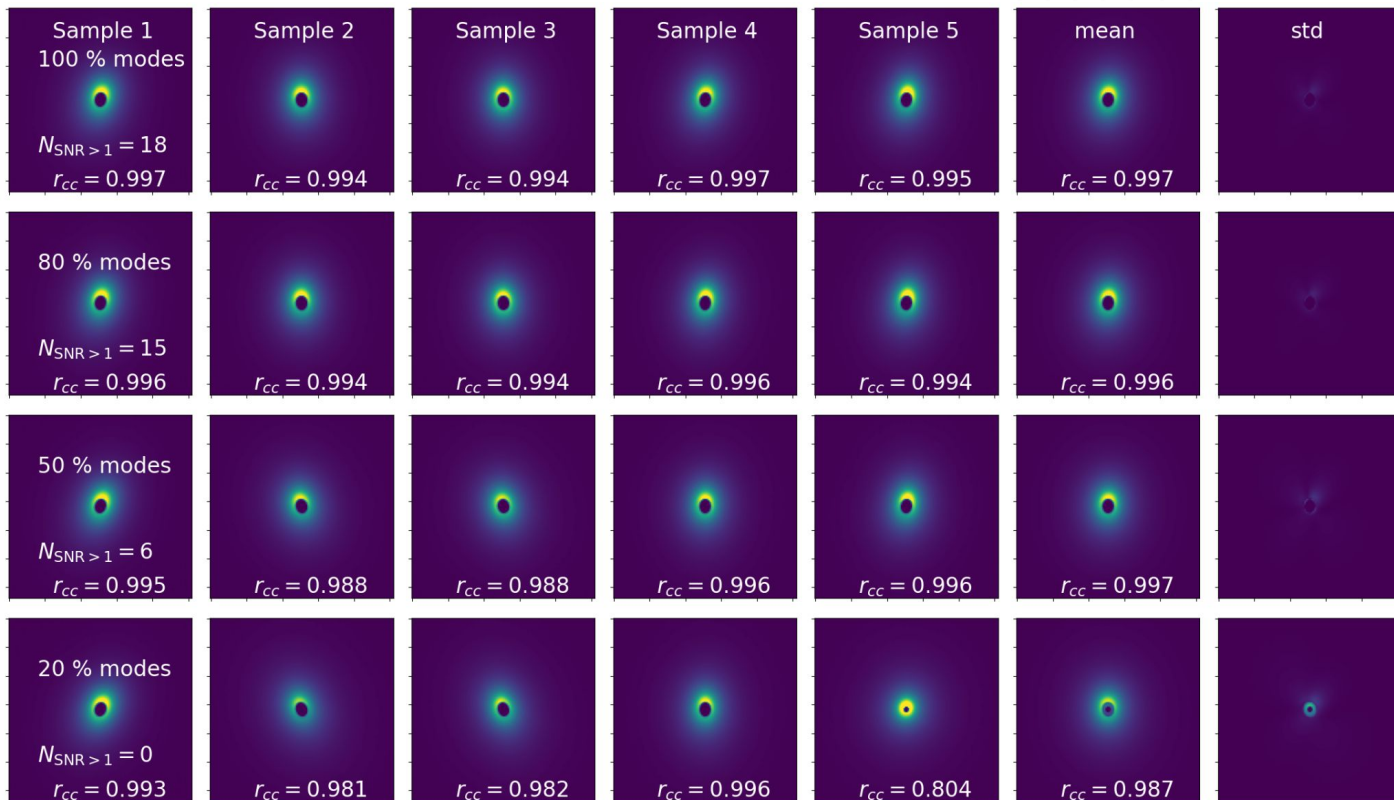
On GRMHD simulations

- ▷ GRMHD simulations of RIAF (Wong et al. 2022)

- ▷ The algorithm is also able to reconstruct small-scale features like rings and spirals, given sufficient SNR (fixed at $\sigma_{|V|^2}=10^{-4}$ here) and good UV coverage.
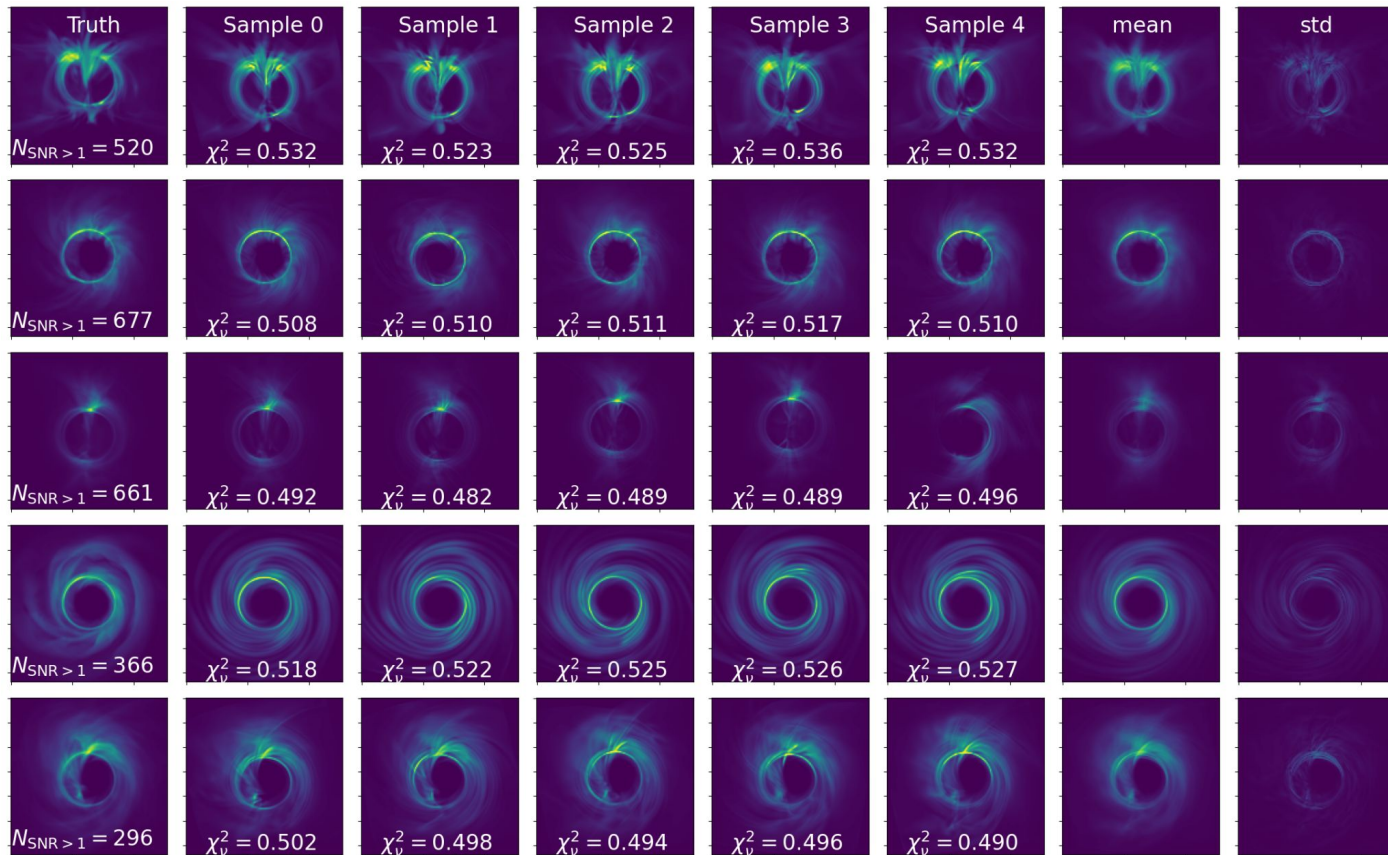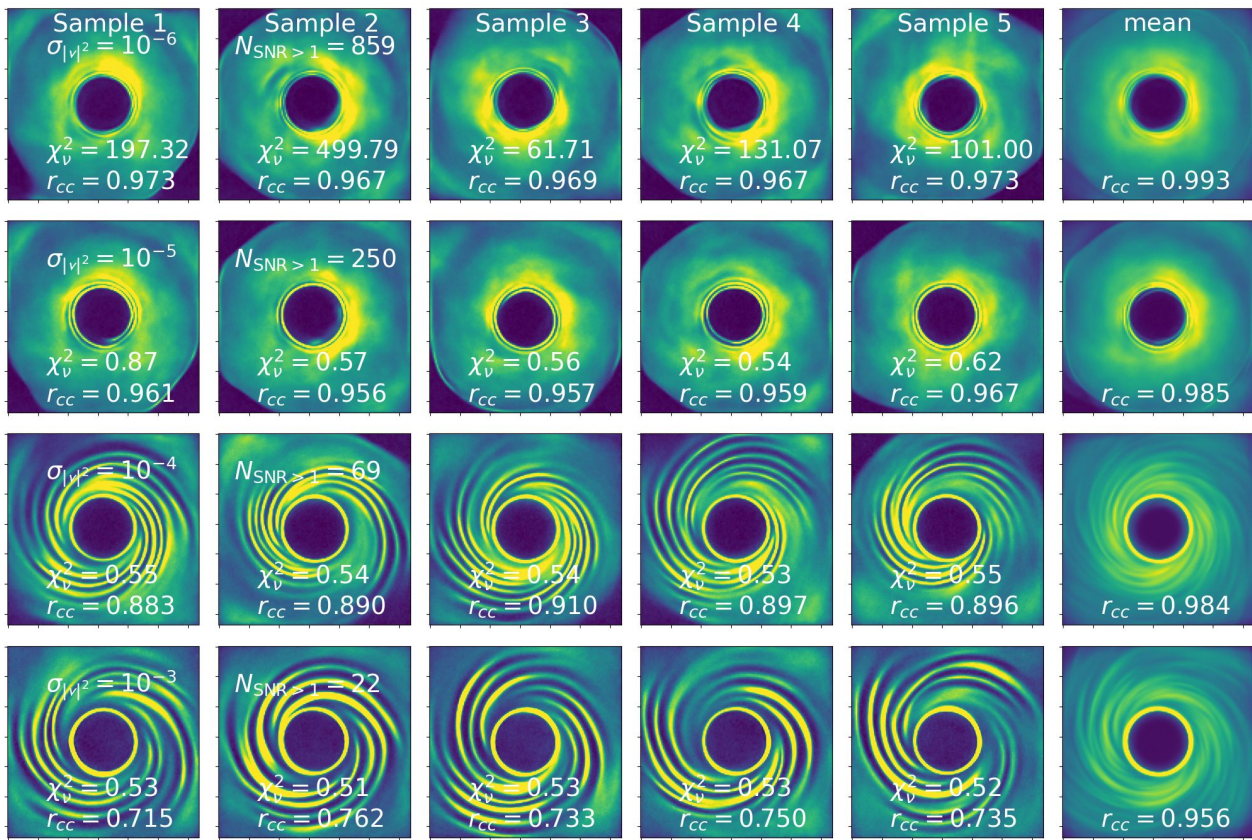
Misspecified prior

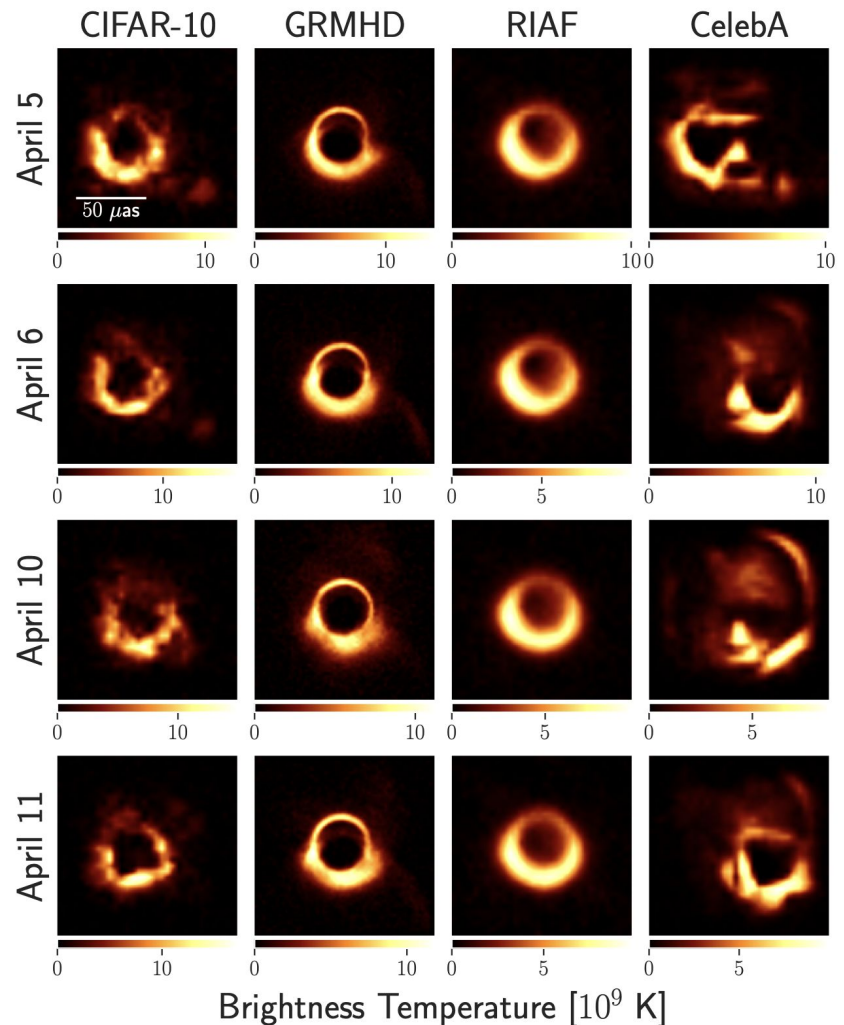- ▷ Reconstruct Shakura-Sunyaev disk with photon ring GRMHD prior.

- ▷ Misspecified prior introduces bias (e.g., spirals, rings) into the images. The reconstruction is a competition between the likelihood (measurement) and the misspecified prior, depending on the SNR.

- ▷ As the noise increases, the reconstructions show more features from the prior. Some features like spirals are random and averaged to 0 in posterior mean.


Truth

	Sample 1	Sample 2	Sample 3	Sample 4	Sample 5	mean
Row 1	$\sigma_{|v|^2} = 10^{-6}$ $\chi_\nu^2 = 197.32$ $r_{cc} = 0.973$	$N_{SNR>1} = 859$ $\chi_\nu^2 = 499.79$ $r_{cc} = 0.967$	$\chi_\nu^2 = 61.71$ $r_{cc} = 0.969$	$\chi_\nu^2 = 131.07$ $r_{cc} = 0.967$	$\chi_\nu^2 = 101.00$ $r_{cc} = 0.973$	$r_{cc} = 0.993$
Row 2	$\sigma_{|v|^2} = 10^{-5}$ $\chi_\nu^2 = 0.87$ $r_{cc} = 0.961$	$N_{SNR>1} = 250$ $\chi_\nu^2 = 0.57$ $r_{cc} = 0.956$	$\chi_\nu^2 = 0.56$ $r_{cc} = 0.957$	$\chi_\nu^2 = 0.54$ $r_{cc} = 0.959$	$\chi_\nu^2 = 0.62$ $r_{cc} = 0.967$	$r_{cc} = 0.985$
Row 3	$\sigma_{|v|^2} = 10^{-4}$ $\chi_\nu^2 = 0.53$ $r_{cc} = 0.883$	$N_{SNR>1} = 69$ $\chi_\nu^2 = 0.54$ $r_{cc} = 0.890$	$\chi_\nu^2 = 0.54$ $r_{cc} = 0.910$	$\chi_\nu^2 = 0.53$ $r_{cc} = 0.897$	$\chi_\nu^2 = 0.55$ $r_{cc} = 0.896$	$r_{cc} = 0.984$
Row 4	$\sigma_{|v|^2} = 10^{-3}$ $\chi_\nu^2 = 0.53$ $r_{cc} = 0.715$	$N_{SNR>1} = 22$ $\chi_\nu^2 = 0.51$ $r_{cc} = 0.762$	$\chi_\nu^2 = 0.53$ $r_{cc} = 0.733$	$\chi_\nu^2 = 0.53$ $r_{cc} = 0.750$	$\chi_\nu^2 = 0.52$ $r_{cc} = 0.735$	$r_{cc} = 0.956$

Misspecified prior

▷ Feng et al. 2024 [2406.02785] explores reconstructing EHT images with different priors:
  ○ CIFAR-10: natural images like cars, airplanes, animals, etc.
  ○ GRMHD photon-ring simulations
  ○ Radiatively Inefficient Accretion Flow (RIAF) models
  ○ CelebA: Celebrity faces

▷ Different (misspecified) priors introduce different biases, but there are robust features that do not depend on the choice of prior, e.g., ring structure, orientation, asymmetry, etc.

Misspecified prior

▷ Feng et al. 2024 [2406.02785] explores reconstructing EHT images with different priors:
  ○ CIFAR-10: natural images like cars, airplanes, animals, etc.
  ○ GRMHD photon-ring simulations
  ○ Radiatively Inefficient Accretion Flow (RIAF) models
  ○ CelebA: Celebrity faces

▷ Different (misspecified) priors introduce different biases, but there are robust features that do not depend on the choice of prior, e.g., ring structure, orientation, asymmetry, etc.

▷ The CIFAR-10 prior introduces the least amount of noise, because it covers a wide range of natural images (even though none of them look like a ring or a disk).

19
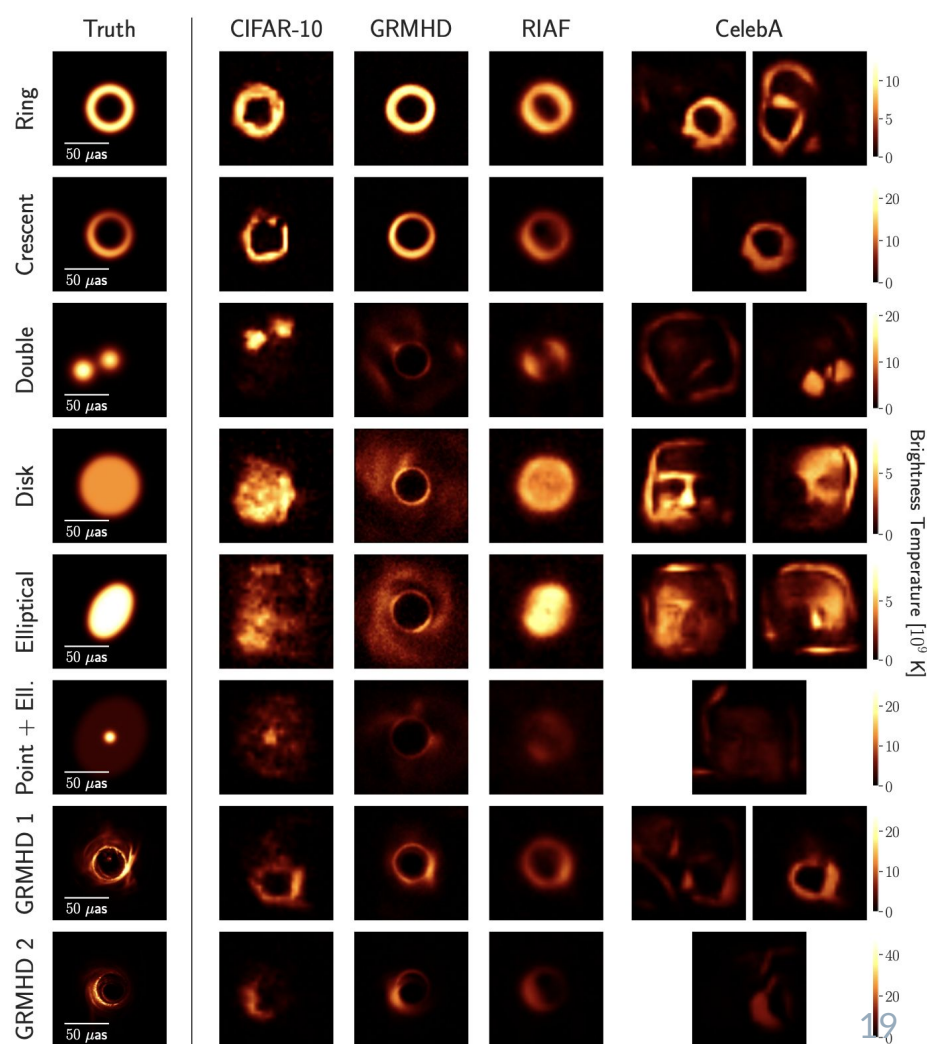
Conclusions

▷ Phase retrieval (reconstructing the image from Fourier amplitude measurement) is possible.

▷ Solving the phase retrieval in a Bayesian framework allows
  ○ Incorporation of measurement uncertainty
  ○ Posterior sampling for uncertainty quantification

▷ Deep generative diffusion models learn the prior distribution from simulations or models.

▷ Misspecified prior may introduce biases into the phase retrieval, but it can be reduced with broad prior choices and high SNR measurements.